A First-Principles Study of Carbon–Oxygen Bond Scission in Multiatomic Molecules on Flat and Stepped Metal Surfaces

Yong-Hui Zhao, Jin-Xun Liu, Hai-Yan Su,* Keju Sun, and Wei-Xue Li*[a]

Step sites over terrace sites have been suggested to be the active sites in many catalytic reactions particularly bond breaking of diatomic molecules. Aiming to provide insight into the role of step sites in multiatomic molecules bond breaking reactions and their dependence on catalysts, we present herein a systematic first-principles study of carbon–oxygen bond scission of diatomic CO and multiatomic HCO and CH$_3$HCO on flat and stepped Co, Rh, and Ir surfaces. We find that multiatomic molecules exhibit distinct carbon–oxygen scission activity from diatomic molecules regardless of the metal catalysts (Co, Rh, and Ir) considered: compared to the huge enhancement of step sites for CO with a barrier 0.81–1.29 eV lower than that of flat surfaces, the role of step sites for CH$_3$CHO is substantially weakened with a barrier 0.11–0.27 eV higher than that of flat surfaces. The reason for this is the change of adsorption configurations on flat surfaces and increase of Pauli repulsion on the congested stepped sites for the dissociation of multiatomic molecules.

Introduction

Since Boudart's classification of reactions in terms of their structure sensitivity or structure insensitivity,[1] the understanding of the structure dependence of reactions has progressed enormously.[1–2] Among them, the bond-breaking reactions of a number of diatomic molecules have been demonstrated to have a greater activity on the surface defects such as step sites than on the flat surfaces.[2] For instance, Zambelli et al. showed that at room temperature, the NO dissociation is dominated by the step edges present on Ru (0001) by scanning tunneling microscopy (STM).[3] This was theoretically confirmed by Hammer, who showed that the barrier required for NO dissociation on the step edges of Ru(0001) is as low as 0.17 eV.[4] Using STM and DFT calculations, Dahl et al.[2j] found that the rate of N≡N bond breaking on Ru(0001) is at least 9 orders of magnitude slower than that on steps. Zubkov et al.[2p] showed that the CO dissociation on stepped Ru(109) surface occurs at low temperature (450–500 K) compared to that on the flat Ru(0001) surface. The experimental finding was proved by Ciobica and van Santen[2f] based on DFT calculations: the CO dissociation barrier on stepped Ru surface is reduced by 120 kJ mol^{-1} compared to that on the flat Ru(0001) surface.

The high activity of step sites has been attributed to the decrease of bond competition effect, which is caused by the adsorbates sharing bonding with surface atoms at the transition state (TS). The magnitude of the bonding competition effect is suggested to be determined by the reactant valency and metal d occupancy: the bonding competition effect decreases with the adsorbate valency, and increases with the metal d occupancy.[5] Apart from the bonding competition effect, the direct Pauli repulsion attributed to the overlap of wavefunctions is also the main factor that affects the stability of TS. It has been reported that the Pauli repulsion is largely determined by the distance between two reactants. As the distance between the adsorbates at the TSs for the dissociation of diatomic molecules on flat and step surfaces is similar, Pauli repulsion contributions to the activation energy on these surfaces are believed to be very similar.[6]

Despite the numerous studies on the dissociation of diatomic molecules, the structure sensitivity of bond breaking of multiatomic molecules including at least three atoms is less studied. As the adsorption of the large-size molecules in terms of their favorable adsorption site, configuration, and bonding strength may be rather different from that of the smaller ones, a large difference in structure sensitivity could be expected. It remains unclear how the adsorption configuration affects the bond competition effect and Pauli repulsion at the TS of the dissociation of multiatomic molecules, and their dependence on metals.

To address these questions, we present herein a comparative DFT study of carbon–oxygen bond breaking of the prototype molecules with gradual increase in size from CO via HCO to CH$_3$CHO. Both flat and stepped transition-metal surfaces of Group VIIIA elements (Co, Rh, and Ir) are considered. Our calculations reveal that the large molecules such as CH$_3$CHO and HCO exhibit completely different carbon–oxygen bond breaking behavior from the small molecules regardless of the metals

[a] Dr. Y.-H. Zhao, J.-X. Liu, Dr. H.-Y. Su, Dr. K. Sun, Prof. Dr. W.-X. Li
State Key Laboratory of Catalysis
Dalian Institute of Chemical Physics
Chinese Academy of Sciences
Dalian, 116023 (China)
Fax: (+86) 411-8469-4447
E-mail: hysu@dicp.ac.cn
         wxli@dicp.ac.cn
Supporting information for this article is available on the WWW under http://dx.doi.org/10.1002/cctc.201301114.

considered, with similar or even higher barriers on stepped surfaces than that of flat surfaces.

Results and Discussion

Carbon–oxygen bond scission in CO on Co surfaces

The CO dissociation on Co surfaces has been extensively studied by using periodic DFT calculations. For the sake of consistency with respect to calculation parameters, we performed our own calculations for this system. We first studied the diatomic CO dissociation on the flat Co(0001) surface.

CO binds through its C atom perpendicularly at hcp hollow sites, as shown in Figure 1a, with the binding energy of -1.67 eV(Table 1). At the TS, the carbon atom is near the three-
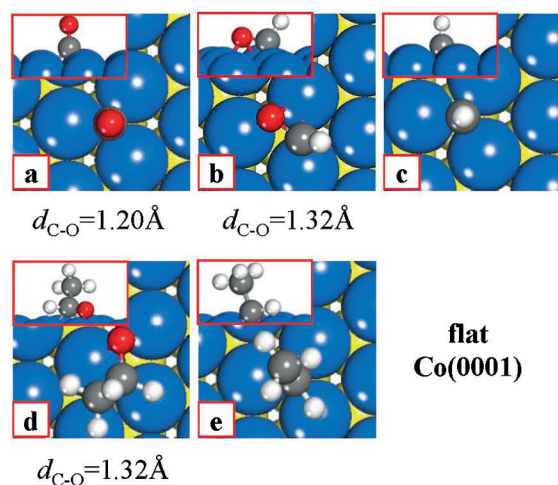
Figure 1. Optimized configuration of the adsorbates at the most stable sites on Co (0001): a) CO; b) HCO; c) CH; d) CH$_3$CHO; e) CH$_3$CH. Gray, red, white, blue, and yellow balls represent carbon, oxygen, hydrogen, and Co atoms on the top and second layer on the flat surface, respectively.
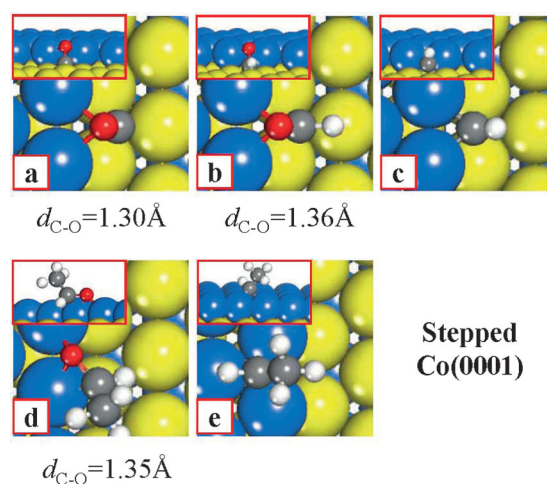
Table 1. Adsorption energy (E_{ads}, eV) with respect to the gaseous radical or molecule and favorable adsorption sites of the various adsorbates on the flat and stepped Co(0001) surface.

Species	Flat Co(0001)		Stepped Co(0001)	
	Site	E_{ads}	Site	E_{ads}
C	hcp	-6.86	step–corner	-7.70
O	hcp	-5.96	near-edge–hcp	-6.27
CO	hcp	-1.67	step–corner	-1.87
CH	hcp	-6.36	step–corner	-6.77
HCO	C$_{bridge}$–O$_{bridge}$	-2.25	step–corner	-2.92
CHCH$_3$	hcp	-3.70	near-edge–hcp	-3.90
CH$_3$CHO	C$_{bridge}$–O$_{bridge}$	-0.54	edge–O$_{bridge}$–C$_{top}$	-1.15

fold hcp hollow site, and oxygen is near a bridge site, sharing a metal atom (Figure 2a). The carbon–oxygen bond length at the TS is 1.83 Å, which manifests itself as a late TS. Correspondingly, the activation barrier is significantly high with a value of 2.37 eV, and the elementary step is endothermic by 0.74 eV, as listed in Table 2.
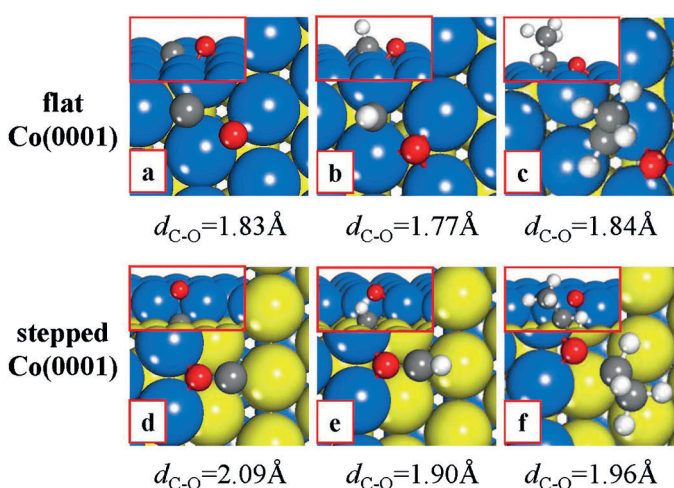
Figure 2. Top view of the TSs of the C—O bond-breaking reactions on flat and stepped Co(0001). a) CO→C+O; b) HCO→CH+O; c) CH$_3$CHO→ CH$_3$CH+O. The blue and yellow balls represent Co atoms on the upper and lower layer on the step, respectively.

Table 2. Calculated activation energies (E_{act}, eV) and reaction energies (ΔH, eV) for C—O bond-breaking reactions on the flat and stepped Co(0001) surfaces.

Reactions	Flat Co(0001)		Stepped Co(0001)	
	E_{act}	ΔH	E_{act}	ΔH
CO→C+O	2.37	0.74	1.39	-0.20
HCO→CH+O	0.71	-0.66	0.73	-0.72
CH$_3$CHO→CH$_3$CH+O	0.72	-0.45	0.99	-0.35

Figure 3. Optimized configuration of the adsorbates at the most stable sites on stepped Co(0001): a) CO; b) HCO; c) CH; d) CH$_3$CHO; e) CH$_3$CH.

On the stepped Co surface, CO binds through both C and O atoms in a tilted configuration at the initial state (IS) with a slightly larger binding energy of -1.87 eV, as shown in Figure 3a. Compared to the perpendicular adsorption of CO on Co(0001) with the carbon–oxygen bond length of 1.20 Å, the

carbon–oxygen bond length of the tilted CO along the step edge is slightly elongated to 1.30 Å. Clearly, CO adsorbed at the tilted configuration is preactivated through the ensemble effect of the step, which would save the energy cost of bond bending required before the dissociation occurs on Co(0001). More importantly, at the TS, the C and O atoms sit on different layers of monatomic steps with carbon–oxygen bond length of 2.09 Å, and no surface Co atoms are shared (Figure 2 b). The bond competition effect on the stepped Co is, therefore, largely reduced, as discussed below. This step is exothermic by −0.20 eV, with an activation energy barrier of only 1.39 eV. The large reduction of the bond breaking barrier for small molecules such as CO on step surfaces is evident, which agrees well with the literature.[2e, g, k, m]

Carbon–oxygen bond scission in HCO on Co surfaces

We then investigated the structure sensitivity of the carbon–oxygen bond scission of a slightly larger molecule, namely HCO. The most favorable structure of adsorption is identified as IS on Co(0001), as shown in Figure 1 b, with a large binding energy of −2.25 eV. Compared to the perpendicular adsorption of CO on Co(0001), a prominent difference for HCO adsorption is that the corresponding carbon–oxygen bond is now parallel to the surface because of the presence of C−H bond. Specifically, both carbon and oxygen of HCO coordinates to surface metal atoms in a so-called bridge–hcp–bridge configuration. The carbon–oxygen bond length of adsorbed HCO is 1.32 Å, similar to that of tilted CO adsorption at the step edge at which both C and O coordinate with surface metal atoms too. This unique structure turns out to be essential for a facile carbon–oxygen bond breaking. The C−H axis slightly rotates from the tilted configuration to the upright configuration during the bond breaking process, and the oxygen moves directly from its initial position (bridge site) to an adjacent hcp–hollow site, sharing one metal atom with CH at the TS (see Figure 2 c). The TS is approached with less extension of the C−O bond (1.77 Å) than in the case of CO activation. The calculated barrier is 0.71 eV and the corresponding reaction energy is −0.66 eV. This is in stark contrast to the demanding barrier and unfavorable reaction energy of CO dissociation on the same surface.

As shown in Figure 3 b, HCO also preferably binds through both C and O on the step, with C at the hcp hollow site of the lower layer and O at the bridge site of the upper layer. The carbon–oxygen axis is inclined by 67.36° from the surface plane, and the C−H axis is almost parallel to the surface. The carbon–oxygen bond length of adsorbed HCO was calculated to be 1.36 Å, and the binding energy is −2.92 eV. Both carbon and oxygen retain their preference in adsorbed HCO molecule in the carbon–oxygen bond scission process. The reaction coordinate is composed of an extension of the carbon–oxygen bond accompanied by a rotation of the C≡H bond. The H−C axis is more tilted at 80.74° from the surface plane than on flat Co(0001), with the H pointing away from the O on the terrace above, the carbon–oxygen bond length is 1.90 Å at the TS (Figure 2 d).

Despite the slightly longer carbon–oxygen bond on stepped Co(0001) surface than on flat Co(0001), there are no surface Co atoms shared by the CH and O at the TS on the step. The calculated barrier is modest with a value of 0.73 eV, and the corresponding reaction energy of this elementary step is −0.72 eV. The similar activity of carbon–oxygen bond scission of HCO on both flat and stepped Co surface is understandable from the structural variation from IS to TS depicted above, but again rather different from the activation of CO molecule.
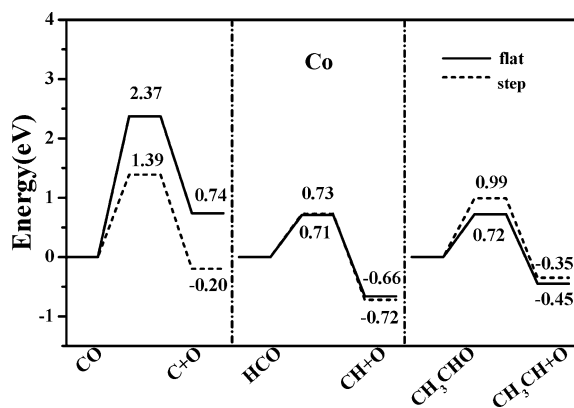
Carbon–oxygen bond scission in CH₃CHO on Co surfaces

We then turned our attention to the bond scission of the largest species CH₃CHO considered herein. CH₃CHO binds through both C and O atoms in a bridge–hcp–bridge configuration on the flat Co(0001) (see Figure 1 d), with the C−O axis nearly parallel to the surface. The carbon–oxygen bond length is 1.36 Å and calculated binding energy for CH₃CHO is −0.54 eV. As the C−O bond is broken, the oxygen moves to a nearby hcp hollow site, sharing one metal atom with carbon. The remaining CH₃CH undergoes a slight rotation, the with C−C axis tilted by 57.38° from the surface plane at the TS (see Figure 2 e). This TS structure also belongs to the "late TS", with a rather long C (in CH)–O distance (1.84 Å). The elementary step is exothermic by −0.45 eV, and the activation energy barrier was calculated to be 0.72 eV. The overall process is very similar to that of HCO activation on same flat surface.

CH₃CHO prefers a C_{top}–O_{bridge} configuration plotted in Figure 3 d on the stepped Co, with the carbon–oxygen bond length of 1.35 Å. The calculated binding energy is −1.15 eV, which is approximately 0.61 eV stronger than that on the flat Co. The trend variation found here agrees with previous experimental results for aldehyde adsorption on open Pd(110) and flat Pd(111).[7] The carbon–oxygen bond scission of CH₃CHO on the stepped Co is exothermic by −0.35 eV, with a higher reaction barrier (0.99 eV) than on the flat Co(0001). There are no surface Co atoms shared by the dissociated fragments at the TS on the stepped Co: O atom binds at the edge–bridge site on the terrace above, and CH₃CH binds through its C atom at the bridge site on the terrace below (Figure 2 (f)). However, the CH₃CH undergoes a larger rotation than on the flat Co(0001) surface, as seen from the C−C angles of 74.32° and 57.38° with respect to the surface plane. As a result, the methyl carbon points away from the O atom at the TS, with a carbon–oxygen distance of 1.96 Å.

Discussions on Co surfaces

The C−O bond scission for diatomic molecule CO is much easier on the stepped Co than on Co(0001). As seen from Table 2, CO dissociation is strongly endothermic on Co(0001) (0.74 eV), whereas the reaction becomes exothermic by −0.20 eV on the stepped Co. Moreover, the calculated barrier on the stepped Co is significantly lower than that on the flat Co(0001) surface (1.39 eV versus 2.37 eV). However, as the size of molecules increases to HCO, the C−O bond scission has a dissociation barrier of 0.73 eV on the stepped Co (see

Figure 4. Energy profiles (barrier and reaction energy) for C–O bond scission reactions on flat (——) and stepped Co(0001) (-----).

Figure 4), which is comparable to that on Co(0001) (0.71 eV). For the larger molecule CH$_3$CHO, the carbon–oxygen bond scission on the stepped Co surface, with a barrier of 0.99 eV, becomes even more difficult than on Co(0001) by 0.27 eV. The reaction energies for carbon–oxygen bond scission in HCO (−0.72 eV) and CH$_3$CHO (−0.35 eV) on the stepped Co are similar to those on flat Co(0001) (−0.66 eV and −0.45 eV), respectively.

First of all, we note that the adsorbed CO binds through both C and O atoms on the stepped Co in a tilted configuration, clearly distinct from the case on the flat Co(0001) surface on which CO binds only through its C end. No bond bend is demanded before the dissociation occurs on the stepped Co. Furthermore, the carbon–oxygen bond length on the stepped Co is elongated by 0.10 Å compared with that on Co (0001), suggesting that CO is preactivated on the step and contributes to the decrease in the activation barrier. However, the multiatomic molecules HCO and CH$_3$CHO bind through both C and O atoms regardless of the surface structures, and carbon–oxygen bond is preactivated on both flat and stepped Co. It is interesting to compare the barrier of CO dissociation and HCO/CH$_3$CHO dissociation on flat Co(0001) (Figure 4). We found that the HC–O and CH$_3$HC–O have dissociation barriers of 0.71 and 0.72 eV, significantly lower than that of carbon–oxygen dissociation (2.37 eV). Compared to the bond length of adsorbed CO of 1.20 Å, the carbon–oxygen bond in HCO and CH$_3$CHO is elongated by 0.12 and 0.16 Å. In contrast, at TS, the carbon–oxygen length for HCO (1.77 Å) and CH$_3$CHO (1.84 Å) dissociation is similar to that for CO dissociation (1.83 Å). These results imply that the low HC–O and CH$_3$HC–O dissociation barrier can be attributed to the preactivation of carbon–oxygen bond in their initial adsorption configuration to a large extent. The presence of CH$_3$ and H can also have an influence on the carbon–oxygen bond scission. However, the effect is relatively small, as seen from the similar barriers between HC–O (0.71 eV) and CH$_3$HC–O dissociation (0.72 eV).

To reveal the origin of the different bond-breaking behavior between the diatomic and multiatomic molecules, we performed a systematic analysis of the activation energies. As the activation energy is the energy difference between the ISs and

TSs, we will address the corresponding geometric and energetic features of the states, respectively. As listed in Table 1, the stepped Co binds all species stronger than the flat Co surface, and the extent of the stabilization increases in size from 0.20 eV for CO to 0.67 and 0.61 eV for HCO and CH$_3$CHO, respectively. The larger stabilization role of the step edge for multiatomic molecules adsorption at the ISs will leave less room to take further advantage of the following bond scission, as indeed found above.

We then decomposed the total energy of the dissociated fragments A and B at the TS, E_{A+B}^{TS},[4] into the chemisorption energy of each fragment at the TS (E_A^{TS}, E_B^{TS}) and the interaction energy between the fragments at the TS, E_{int}^{TS}, which consists mainly of two parts: 1) the bonding competition effect, which is caused by fragments sharing bonding with surface atoms[5,6] and 2) the direct Pauli repulsion between fragments owing to overlap of wave functions.

For CO dissociation, no surface Co atoms are shared by the C and O atoms at the TS on stepped Co. Furthermore, the C and O atoms are located on different layers of monatomic steps, and no overlap exists between the fragments, thereby the E_{int}^{TS} is largely decreased compared to that on the flat Co(0001) surface (0.10 eV versus 0.62 eV). In addition, the E_C^{TS} and E_O^{TS} also contribute a large portion to the barrier decrease between the flat and stepped Co(0001) surface.

Similarly to carbon–oxygen dissociation of CO, no surface Co atoms are shared by the dissociated fragments at the TS for HC–O and CH$_3$HC–O dissociation on the stepped Co. The bonding competition effect between the dissociated fragments on the stepped Co is thus weakened with respect to the flat surface. However, considering the geometric structure of step sites, the distance between the dissociated O and H of CH is substantially decreased, and thereby leading to large direct Pauli repulsion owing to overlap of wave functions. For instance, for HC–O, dissociation on the stepped Co is decreased by only 0.28 eV compared to that on the flat Co, in contrast with the large decrease of E_{int}^{TS} by 0.52 eV between the two surfaces for CO dissociation, indicating a strong direct Pauli repulsion between H and O atom on the stepped Co. For larger CH$_3$HC–O dissociation on the stepped Co, the Pauli repulsion is so strong that CH$_3$ preferably rotates away from O at the upper layer, as seen from the C–C angle of 74.32° with respect to the surface plane, compared with that of 57.38° on flat Co(0001). The rotation also destabilizes the fragments binding at the TS, with the binding energy of CH$_3$CH and O decreased by 0.18 eV and 0.30 eV compared to that on flat Co(0001). As a result, the multiatomic molecules have similar or even higher dissociation barriers on the stepped Co than on the flat Co. This is in stark contrast to diatomic molecule dissociation, the dissociation barriers of which on the stepped surface are approximately one electron volt lower than that on the flat one.

The calculations above were performed by using a standard DFT–GGA functional not accounting for long-range van der Waals (vdW) interactions between the molecule and the surface. It has been demonstrated that metal surfaces that are highly polarizable can lead to significant vdW attraction of adsorbed species,[8] which may have important influence on the

Table 3. Comparison of adsorption energy E_X (X = CO or CH₃CHO) and activation energy E_a (eV) between traditional and optPBE–vdW (in brackets, eV) calculations for CO and CH₃CHO dissociation on flat and stepped Co surfaces.

Surface	CO→C+O		CH₃CHO→CH₃CH+O	
	E_{CO}	E_a	E_{CH_3CHO}	E_a
flat Co	−1.67 (−1.73)	2.37 (2.28)	−0.54 (−0.95)	0.72 (0.66)
stepped Co	−1.87 (−1.99)	1.39 (1.33)	−1.15 (−1.51)	0.99 (0.77)

Figure 5. Energy profiles for C–O bond scission reactions on flat (——) and stepped (-----) a) Rh and b) Ir surfaces.

structures and stabilities of molecules adsorbed on metal surfaces.[8,9] To observe the influence of vdW interactions on the above results, we used the optPBE–vdW method[9a,e] as implemented in the VASP code (VASP 5.3 version) to study the adsorption and dissociation of CO and CH₃CHO on flat and stepped Co (0 0 0 1) surfaces, as listed in Table 3.

Including vdW interaction, both flat and stepped Co(0001) surfaces bind the molecules more strongly than obtained by traditional DFT–PW91 calculations, in agreement with previous calculations. In particular, CH₃CHO exhibits a relatively large enhancement in binding strength, by 0.41 and 0.36 eV on the flat and stepped Co(0001) surfaces, different from that by 0.06 and 0.12 eV for CO, respectively. Additionally, the carbon–oxygen dissociation barriers on both the flat and stepped surfaces decrease by 0.09 and 0.06 eV for CO, and 0.06 and 0.22 eV for CH₃CHO, respectively. Decrease of the barriers could be attributed to the larger extent of weakening of the carbon–oxygen bond of the adsorbates induced by their stronger binding. In addition, the pronounced decrease of CH₃CHO dissociation barrier on the stepped Co might originate from the larger compensation effect of vdW interaction on its stronger steric repulsion. Nevertheless, as seen clearly from Table 3, even after inclusion of the vdW interaction, the CH₃CHO dissociation barrier on the stepped Co (0.77 eV) remains higher than that on the flat one (0.66 eV), whereas CO dissociation barrier on the stepped Co (1.33 eV) remains approximately 1 eV lower than that on the flat one (2.28 eV). In other words, the inclusion of vdW interaction has little influence on the trend variation found by normal DFT–PW91 calculation, which was used in the following for other metal surfaces, accordingly.

C—O bond scission on Rh and Ir surfaces

We perform similar calculations for carbon–oxygen bond scission in CO, HCO, and CH₃CHO on flat and stepped Rh(111) and Ir(111) surfaces (Figure 5). The adsorption energies, activation energies, and the geometry of various intermediates are listed in Table 4 and 5, respectively.
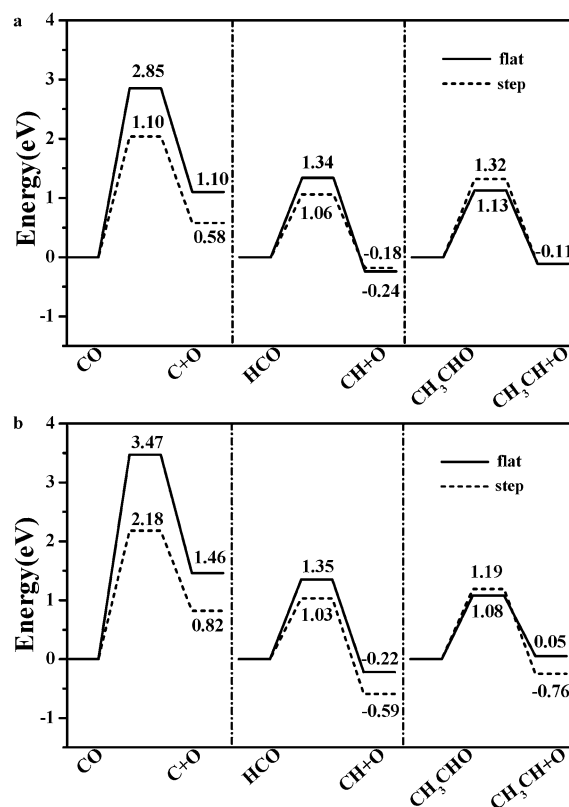
Table 4. Adsorption energy E_{ads} (eV) with respect to that of the gaseous radical or molecule and favorable adsorption sites of the various adsorbates on flat and stepped Rh(111) and Ir(111) surfaces.

Species	Flat Rh		Stepped Rh		Flat Ir		Stepped Ir	
	Site	E_{ads}	Site	E_{ads}	Site	E_{ads}	Site	E_{ads}
C	hcp	−7.40	step–corner	−7.80	hcp	−7.16	step–corner	−7.52
O	fcc	−5.41	edge–bridge	−5.61	fcc	−5.13	edge–bridge	−5.99
CO	hcp	−2.02	edge–bridge	−2.11	top	−1.87	step–top	−2.45
CH	hcp	−6.84	near-edge–hcp	−6.89	hcp	−6.88	near-edge–hcp	−7.14
HCO	CbOhHf[a]	−2.62	edge–tbt[b]	−2.92	tbt	−2.40	edge–tbt	−3.15
CHCH₃	hcp	−4.02	edge–bridge	−4.26	bridge	−3.81	edge–bridge	−4.70
CH₃CHO	CbOfHh	−0.65	edge–O$_{bridge}$–C$_{top}$	−1.09	CbOfHh	−0.32	edge–O$_{bridge}$–C$_{top}$	−1.26

[a] CbOhHf indicates that H is above an fcc site, C is above a bridge site, and O is between an fcc and a top site; [b] tbt indicates that C and O is above neighbouring two top sites.

Table 5. Calculated activation energies (E_{act}, eV) and reaction energies (ΔH, eV) on flat and stepped Rh and Ir(111) surfaces.

surface	CO→C+O		HCO→CH+O		CH₃CHO→CH₃CH+O	
	E_{act}	ΔH	E_{act}	ΔH	E_{act}	ΔH
Rh	2.85	1.10	1.34	−0.24	1.13	−0.11
stepped Rh	2.04	0.58	1.06	−0.18	1.32	−0.11
Ir	3.47	1.46	1.35	−0.22	1.08	0.05
stepped Ir	2.18	0.82	1.03	−0.59	1.19	−0.25

The Rh and Ir surfaces follow exactly the same trend as Co surfaces: the step sites are favorable for the carbon–oxygen bond scission in small molecule such as CO, however, the pref-

erence decreases significantly for larger molecules HCO and CH$_3$CHO. As seen from Table 5, CO dissociation has activation energy barriers of 2.04 and 2.18 eV on the stepped Rh and Ir surfaces, largely lower than the corresponding values (2.85 and 3.47 eV) on the flat surfaces. Furthermore, the reaction on the stepped Rh and Ir surfaces is less endothermic than on the flat surfaces by 0.52 and 0.64 eV. If the size of molecules increases to HCO, the dissociation barriers are slightly lower on stepped Rh(111) and Ir(111) surfaces than on corresponding flat surfaces (by 0.28 and 0.32 eV). For larger molecules, CH$_3$CHO, the carbon–oxygen bond scission has the activation energy barriers of 1.32 eV and 1.19 eV on the stepped Rh(111) and Ir(111) surfaces, higher than those on the corresponding flat surfaces by 0.19 eV and 0.11 eV, respectively. Because of the similarities between the Co, Rh, and Ir surfaces, the analysis of the reaction barriers in carbon–oxygen bond breaking on Rh and Ir surfaces can be seen similar to those on Co surfaces. More energetic and structure information can be found in the Supporting Information.

By careful comparison, we found that Co has a higher activity toward carbon–oxygen bond breaking than Rh and Ir regardless of the surface structure. This reflects the difference of the intrinsic activity of metals. Interestingly, the high activity of Co also leads to its unique CO adsorption configuration: CO binds through both C and O atoms in a tilted configuration on the stepped Co (Figure 3a), which is clearly distinct from the perpendicular configuration on stepped Rh and Ir (Figure S2a and S4a). These results reveal that the oxophilicity of Co is so strong that the energy gain owing to the Co–O bond formation exceeds the energy cost with the C–O bond tilted. The higher activity of 3d transition metals than of 4d and 5d transition metals has also been addressed in Ref. [10] and [11].

Discussions on the overall activity

As shown in the literature and herein, the step sites can greatly enhance diatomic molecules such as CO, N$_2$, and NO dissociation.[2c, i,j, 12] This is owing to the fact that the step sites have a smaller bond competition effect at the TS, thereby lower activation energy barrier and higher activity. However, the dissociation of multiatomic molecules exhibits a distinct feature from that of diatomic molecules. On the step sites, the direct Pauli repulsion plays a dominant role in the TS stability regardless of the metals considered. The fragments preferably rotate away from each other to weaken the repulsive interaction at the TS, which, in turn, destabilizes the fragments binding. The dissociation barriers for the multiatomic molecules are slightly lower (HCO dissociation) or even higher (CH$_3$CHO dissociation) on the stepped than on the flat surface regardless of the metal considered.

Apart from the activation energy barriers, the reaction rate also depends on the equilibrium constants of reactants determined by their adsorption energies. To estimate the reaction rate by taking into account both contributions, we consider the following elementary reaction steps, adsorption from the gas phase [Eq. (1)] and subsequent dissociation on the surface [Eq. (2)]:

$$AB_{(g)} + * = AB* \tag{1}$$

$$AB* + * = A* + B* \tag{2}$$

For the metals we consider herein, Equation (1) is unactivated and fast, and we assume that the reaction is in equilibrium applying at the higher temperature. Corresponding equilibrium constants K_1 is determining by the adsorption energy as detailed in the Supporting Information. For Equation (2), rate constant k_2 for a forward reaction is shown in Equation (3):

$$k_2 = A \exp(-E_a/kT) \tag{3}$$

in which A is a prefactor, E_a is the activation energy, k is the Boltzmann constant, and T is the absolute temperature. Therefore, the overall forward reaction rate r for dissociation at a given partial pressure P could be evaluated approximately by Equation (4):

$$r = k_2 K_1 P/(1 + K_1 P)^2 \tag{4}$$

In Table 6, a comparison of the reaction rate on flat and stepped Co surfaces is shown. The reaction rate is calculated at $T = 500$ K, $P = 10^{-2}$ Pa, corresponding to low-pressure condi-

Table 6. Reaction equilibrium constants (K_1), rate constants (k_2, s^{-1}), and reaction rates (r, site^{-1} s^{-1}) for the elementary reaction used in the microkinetic model.

Reactions	K_1	k_2	r
Flat Co(0001)			
CO→C+O	1.7×10^2	1.3×10^{-11}	2.9×10^{-12}
CH$_3$CHO→CH$_3$CH+O	3.4×10^{-13}	5.5×10^5	1.9×10^{-9}
Stepped Co(0001)			
CO→C+O	1.8×10^4	9.6×10^{-2}	5.2×10^{-4}
CH$_3$CHO→CH$_3$CH+O	4.8×10^{-7}	1.0×10^3	5.0×10^{-6}

tions. It can be seen that diatomic C–O dissociation on stepped Co is approximately eight orders of magnitude faster (5.2×10^{-4} vs. 2.9×10^{-12} s^{-1}) than on the flat Co(0001). The high CO dissociation rate on the step originates mainly from the nine orders of magnitude larger k_2 (9.6×10^{-2} vs. 1.3×10^{-11} s^{-1}) for its much lower dissociation barrier. For multiatomic CH$_3$HC–O dissociation on the step, in contrast, the corresponding k_2 is two orders of magnitude smaller k_2 (1.0×10^3 vs. 5.5×10^5 s^{-1}) for its higher dissociation barrier. The reversal of relative k_2 between step and flat sites would suppress completely the preference on the step. On the other hand, we note that larger enhancement of CH$_3$HCO binding strength on the step by 0.61 eV leads to six orders of magnitude increase of corresponding equilibrium constant K_1, compared to only two orders of magnitude increase of K_1 for CO adsorption on the step because of the relatively smaller enhancement of binding strength by 0.20 eV. As a result, the overall reaction rate r for CH$_3$HC–O dissociation on the step remains three orders of magnitude higher (5.0×10^{-6} vs. 1.9×10^{-9} site^{-1} s^{-1})

than that on the terrace. Compared to CO dissociation, with eight orders of magnitude larger reaction rate at the step sites, the role of step in the dissociation of multiatomic molecules was indeed weakened dramatically. Considering the lower fraction of step sites than terrace sites on metal catalysts, the preference of steps in the dissociation of multiatomic molecules would be further reduced. This conclusion is corroborated by the absence of experimental findings for the structure sensitivity of multiatomic molecules bond breaking on metal surfaces.

It is also interesting to compare the difference of dissociation activity between CO and CH_3HCO on given metal surfaces as well as the dependence on the flat and step surfaces. From Table 6, it can be seen that on flat Co surfaces, the reaction rate for CH_3HCO dissociation (1.9×10^{-9} site^{-1}s^{-1}) is three orders of magnitude higher than for CO dissociation (2.9×10^{-12} site^{-1}s^{-1}). The higher reaction rate for CH_3HCO dissociation than that for CO dissociation comes from the significantly higher k_2 and/or lower dissociation barrier (0.72 eV for CH_3HCO vs. 2.37 eV for CO). In contrast, on the stepped Co surfaces, the corresponding barrier for CH_3HCO dissociation increases by 0.27 eV, but decreases by 0.98 eV for CO dissociation. As a result, the reaction rate for CO dissociation (5.2×10^{-4} site^{-1}s^{-1}) becomes two orders of magnitude higher than that of CH_3HCO (5.0×10^{-6} site^{-1}s^{-1}). Namely, the order of dissociation activity between diatomic molecules and multiatomic molecules is also dependent on the surface structures.

Conclusions

The structure sensitivity of carbon–oxygen bond scission of diatomic CO and multiatomic HCO and CH_3HCO on flat and stepped Co(0001), Rh(111), and Ir(111) surfaces was studied systematically by using DFT calculations. Compared to diatomic CO on flat surfaces, the carbon–oxygen bond of multiatomic HCO and CH_3HCO changes from an upright configuration to parallel configuration with respect to the substrates underneath, which facilitates greatly the corresponding bond-breaking process with a lower barrier. The dissociation barrier at step sites decreases significantly for diatomic CO by 0.87–1.27 eV compared to that at terrace sites, and modestly for multiatomic HCO by 0.02–0.32 eV, but increases for CH_3CHO by 0.11–0.27 eV, owing to the gradually increasing of Pauli repulsion at the congested stepped sites.

The microkinetic analysis revealed that the order of dissociation activity between diatomic molecules and multiatomic molecules is dependent on the surface structures, namely, on flat surfaces, multiatomic molecules have a higher bond-breaking activity than diatomic molecules, but reversed on stepped surfaces. Independent on the diatomic and multiatomic molecules, the absolute reaction rate on stepped surfaces is higher than that on flat surfaces. Nevertheless, the relative higher activity for multiatomic molecules on flat surfaces suppresses the extent of the corresponding preference on stepped surfaces. The results obtained provide valuable insights for rationales of the metal catalyst design for the multiatomic molecules activation.

Computational Methods

All calculations were performed by using Vienna ab initio simulation package (VASP),[12] using projector-augmented wave method developed by Blöchl[13] to describe the electron–ion interactions. The Kohn–Sham equations in a plane wave basis set with kinetic energy 400 eV and density cutoff 650 eV are included in the calculation. Generalized gradient approximation in form of the functional proposed by Perdew and Wang,[14] usually referred to as (GGA–PW91),was used to describe the exchange–correlation energy and potential. We have also used VASP 5.3 code to perform the optPBE–vdW calculations,[8a, e] and Perdew–Burke–Ernzerhof (PBE) exchange–correlation functionals[15] were adopted. Spin-polarized calculations were performed throughout the present work for the ferromagnetic nature of Co. The optimized lattice constants are $a = 2.49$ Å and $c = 4.03$ Å for Co, $a = 3.85$ and 3.88 Å for face-centered cubic (fcc) Rh and Ir, respectively.

The flat pristine closed-packed surfaces were simulated by four layers with nine metal atoms per layer representing p(3×3) (corresponding 1/9 ML of surface coverage) surface. Stepped surface were modeled deriving from a four-layer p(7×3) close-packed surface, in which three neighboring rows of metal atoms on the top layer are removed. A vacuum region of 15 Å between any two repeated slabs was found to be sufficient to avoid interactions between repeated slabs along z-direction. The surface Brillouin zone was sampled with a (3×3×1) and (2×5×1) k-point grid generated automatically by using the Monkhorst–Pack method for flat and stepped surfaces.[16] A (15 Å×15.25 Å×15.5 Å) unit cell for isolated gas-phase molecules and atoms were performed and the Brillouin zone was sampled with one k-point.

Geometry optimizations of adsorbates were stopped when the difference in the forces were less than 0.03 eVÅ^{-1}. Adsorption was only allowed on one side of the metal slabs corrected with a dipole moment. The chemisorbed species and metal atoms of the uppermost two layers were allowed to relax till the convergence criterion based on the forces acting on the atoms, while the remained atoms were fixed at their bulk truncated positions. Increasing the slab thickness to five layers was found to decrease the adsorption energies of intermediates by less than 0.1 eV and has an even smaller effect on calculated barriers. Thus, the four-layer slab model was sufficient.

All TSs were located by an efficient constrained minimization method,[17] and the relaxation would stop until the residual forces in each atom were smaller than 0.03 eVÅ^{-1}. The elementary activated barrier was calculated with respect to the most stable adsorption on the surfaces. We also located the TSs of some of the minimum energy reaction pathways by the climbing-image nudged-elastic-band method.[18] The TS structures located by the two methods were very similar, implying the reliability of constrained minimization method in searching the TS. Frequency calculations revealed that in all cases only a single imaginary frequency is obtained, which means that the TSs found are true saddle points on the potential energy surface.

Acknowledgements

[1] M. Boudart, F. Rumpf, *React. Kinet. Catal. Lett.* **1987**, *35*, 95–105.
[2] a) S. Shetty, R. A. van Santen, *Top. Catal.* **2010**, *53*, 969–975; b) Z. P. Liu, S. J. Jenkins, D. A. King, *J. Am. Chem. Soc.* **2003**, *125*, 14660–14661; c) J. Rempel, J. Greeley, L. B. Hansen, O. H. Nielsen, J. K. Norskov, M. Mavrikakis, *J. Phys. Chem. C* **2009**, *113*, 20623–20631; d) P. Crawford, P. Hu, *Surf. Sci.* **2007**, *601*, 341–345; e) Q. Ge, M. Neurock, *J. Phys. Chem. B* **2006**, *110*, 15368–15380; f) I. M. Ciobica, R. A. van Santen, *J. Phys. Chem. B* **2003**, *107*, 3808–3812; g) S. Shetty, A. P. J. Jansen, R. A. van Santen, *J. Phys. Chem. C* **2008**, *112*, 14027–14033; h) T. Zubkov, G. A. Morgan, J. T. Yates, *Chem. Phys. Lett.* **2002**, *362*, 181–184; i) M. Mavrikakis, M. Baumer, H. J. Freund, J. K. Norskov, *Catal. Lett.* **2002**, *81*, 153–156; j) S. Dahl, A. Logadottir, R. C. Egeberg, J. H. Larsen, I. Chorkendorff, E. Tornqvist, J. K. Norskov, *Phys. Rev. Lett.* **1999**, *83*, 1814; k) X. F. Ma, H. Y. Su, H. Q. Deng, W. X. Li, *Catal. Today* **2011**, *160*, 228–233; l) B. Hammer, *Phys. Rev. Lett.* **1999**, *83*, 3681; m) A. Stroppa, F. Mittendorfer, J. N. Andersen, G. Parteder, F. Allegretti, S. Surnev, F. P. Netzer, *J. Phys. Chem. C* **2009**, *113*, 942–949; n) G. Ertl, *Philos. Trans. R. Soc. London* **2005**, *363*, 955–958; o) G. R. Darling, S. Holloway, *Rep. Prog. Phys.* **1995**, *58*, 1595–1672; p) T. Zubkov, G. A. Morgan, Jr., J. T. Yates, Jr., O. Kühlert, M. Lisowski, R. Schillinger, D. Fick, H. J. Jänsch, *Surf. Sci.* **2003**, *526*, 57–71; q) H. Wang, W. Zhou, J. X. Liu, R. Si, G. Sun, M. Q. Zhong, H. Y. Su, H. B. Zhao, J. A. Rodriguez, S. J. Pennycook, J. C. Idrobo, W. X. Li, Y. Kou, D. Ma, *J. Am. Chem. Soc.* **2013**, *135*, 4149–4158; r) J. X. Liu, H. Y. Su, W. X. Li, *Catal. Today* **2013**, *215*, 36–42; s) J. X. Liu, H. Y. Su, D.-P. Sun, B. Y. Zhang, W. X. Li, *J. Am. Chem. Soc.* **2013**, *135*, 16284–16287.
[3] T. Zambelli, J. Wintterlin, J. Trost, G. Ertl, *Science* **1996**, *273*, 1688–1690.
[4] B. Hammer, *Surf. Sci.* **2000**, *459*, 323–348.
[5] Z. P. Liu, P. Hu, *J. Chem. Phys.* **2001**, *114*, 8244–8247.
[6] Z. P. Liu, P. Hu, *J Am Chem. Soc* **2003**, *125*, 1958–1967.
[7] J. Davis, M. Barteau, *J. Am. Chem. Soc.* **1989**, *111*, 1782–1792.
[8] A. Tkatchenko, L. Romaner, O. T. Hofmann, E. Zojer, C. Ambrosch-Draxl, M. Scheffler, *MRS Bull.* **2010**, *35*, 435–442.
[9] a) J. Klimeš, D. R. Bowler, A. Michaelides, *Phys. Rev. B* **2011**, *83*, 195131; b) W. Liu, J. Carrasco, B. Santra, A. Michaelides, M. Scheffler, A. Tkatchenko, *Phys. Rev. B* **2012**, *86*, 245405; c) F. B. de Mongeot, A. Toma, A. Molle, S. Lizzit, L. Petaccia, A. Baraldi, *Phys. Rev. Lett.* **2006**, *97*, 056103; d) V. G. Ruiz, W. Liu, E. Zojer, M. Scheffler, A. Tkatchenko, *Phys. Rev. Lett.* **2012**, *108*, 146103; e) J. Klimes, D. R. Bowler, A. Michaelides, *J. Phys. Condens. Matter* **2010**, *22*, 022201.
[10] M. Gajdoš, A. Eichler, J. Hafner, *J. Phys. Condens. Matter* **2004**, *16*, 1141–1164.
[11] J. K. Nørskov, T. Bligaard, J. Rossmeisl, C. H. Christensen, *Nat. Chem.* **2009**, *1*, 37–46.
[12] a) G. Kresse, J. Hafner, *Phys. Rev. B* **1993**, *48*, 13115–13118; b) G. Kresse, J. Furthmuller, *Phys. Rev. B* **1996**, *54*, 11169–11186; c) G. Kresse, J. Hafner, *Phys. Rev. B* **1993**, *47*, 558–561.
[13] P. E. Blöchl, *Phys. Rev. B* **1994**, *50*, 17953–17979.
[14] a) J. P. Perdew, J. A. Chevary, S. H. Vosko, K. A. Jackson, M. R. Pederson, D. J. Singh, C. Fiolhais, *Phys. Rev. B* **1992**, *46*, 6671–6687; b) Y. Wang, J. P. Perdew, *Phys. Rev. B* **1991**, *44*, 13298.
[15] J. P. Perdew, K. Burke, M. Ernzerhof, *Phys. Rev. Lett.* **1996**, *77*, 3865–3868.
[16] H. J. Monkhorst, J. D. Pack, *Phys. Rev. B* **1976**, *13*, 5188.
[17] K. J. Sun, Y. H. Zhao, H. Y. Su, W. X. Li, *Theor. Chem. Acc.* **2012**, *131*, 1118.
[18] a) G. Henkelman, H. Jonsson, *J. Chem. Phys.* **2000**, *113*, 9978–9985; b) G. Henkelman, B. P. Uberuaga, H. Jonsson, *J. Chem. Phys.* **2000**, *113*, 9901–9904.